Physics of the Earth and Planetary Interiors 293 (2019) 106270

Contents lists available at ScienceDirect

Physics of the Earth and Planetary Interiors

journal homepage: www.elsevier.com/locate/pepi

# Tectono-magmatic characteristics of post-collisional magmatism: Case study East Carpathians, Călimani-Gurghiu-Harghita volcanic range

Ioan Seghedi[a,*], Lucian Besutiu[a], Viorel Mirea[a], Luminita Zlagnean[a], Răzvan-Gabriel Popa[a,b], Alexandru Szakács[a], Ligia Atanasiu[a], Mihai Pomeran[a], Mădălina Vişan[a]

[a] Institute of Geodynamics, Romanian Academy, 19–21, Jean-Luis Calderon Str., Bucharest 020032, Romania
[b] Institute of Geochemistry and Petrology, ETH Zürich, Clausiusstrasse 25, 8092 Zürich, Switzerland

ARTICLE INFO

*Keywords:*
Post-collisional
Volcanism
Transtensional
Extension
Tectonics
Aeromagnetic
Gravity
Geophysics

ABSTRACT

This work provides a comprehensive GIS mapping integrated with geological and geophysical data (magnetic and gravimetric) to reveal the interplay between (i) magmatism and volcanic activity, (ii) intra-mountain basin development and (iii) large-scale faulting/tectonic features in the post-collisional setting of the East Carpathians. The geological, geophysical and tectonic data of the Călimani-Gurghiu-Harghita range (CGH) confirm the contemporaneous formation of basins and volcanic activity. The two phenomena propagated southwards in time, parallel to the collisional front, in close relation to the development of the fault systems. The geometry of the faults and alignment of volcanic edifices indicate both strike-slip and normal faulting, with no rotation. The main volcanic range and main tectonic basins evolved along a regional NNW-SSE striking sinistral transtensional fault zone with left stepping stepovers and pull-apart basins in the transfer areas. The fault zones probably acted as least resistance areas that fostered the development of magma ascent paths and plumbing systems. These connected the volcanic centers with numerous magma chambers emplaced at the upper mantle – lower crust boundary and throughout the lower and upper crust. The magma generation is most likely a result of the interplay between large-scale transtensional systems that induced decompression in the previously metasomatised mantle, and asthenosphere upwelling in the post-collisional East Carpathian orogen.

## 1. Introduction

The post-collisional geodynamic setting is not yet fully integrated in the model of plate tectonics. Even so, many authors recognize that plate collision s.s. (period of maximum convergence) can generate a magmatic source. This source can be either in the crust or in the lithospheric/asthenosperic mantle and the preceding subduction can have an influence on its initial development (e.g., Liegeois, 1998). However, the current knowledge regarding the structural control on "post-collisional volcanism" is poor. It comes in contrast to our much vaster structural understanding of present-day "volcanic arc" systems. The latter benefit from a multitude of studies on the geometry and kinematics of the major tectonic systems responsible for crustal chamber development, rise and extrusion of magma (e.g., Acocella, 2014 and references therein).

Most of the information concerning the post-collisional magmatic activity is derived from petrological studies. For example, the geological evidence that post-collisional magmatic activity is delayed timewise in respect to subduction and convergent processes is approached mainly from a petrological point of view (e.g., Chung et al., 2005; Dilek and Altunkaynak, 2007; Hébert et al., 2014, Zhang et al., 2018, etc.). Such case studies are exemplified in the Alpine–Himalayan belt. Here, following Mesozoic-Tertiary collisional events, a systematic temporal pattern of post-collisional magmatic events is observed. This pattern starts with a dominant acidic ignimbrite flare-up. It is followed by the eruption of a variety of subalkaline, potassic and/or ultrapotassic magmas, which are progressively less voluminous. This suggests a diminishing dehydration and "de-fertilization" of the lithospheric mantle source and is indicative of source modification. In this context, silica-undersaturated sodic-alkaline rocks, suggesting asthenospheric mantle sources are the youngest generated magmas (e.g., Prelević and Seghedi, 2013 and references therein). This shows that the post-collisional magmatism is an intriguing concept that involves very different magmatic sources capable of feeding the same volcanic centers. To further our knowledge, it is important to understand how the magmatic patterns relate to tectonic patterns. This can be achieved by studying relevant case studies, using a combined magmatic-tectonic approach.

The Călimani-Gurghiu-Harghita range (CGH) is a remarkable

* Corresponding author.
*E-mail address:* seghedi@geodin.ro (I. Seghedi).

https://doi.org/10.1016/j.pepi.2019.106270
Received 31 July 2018; Received in revised form 20 March 2019; Accepted 1 June 2019
Available online 04 June 2019
0031-9201/ 

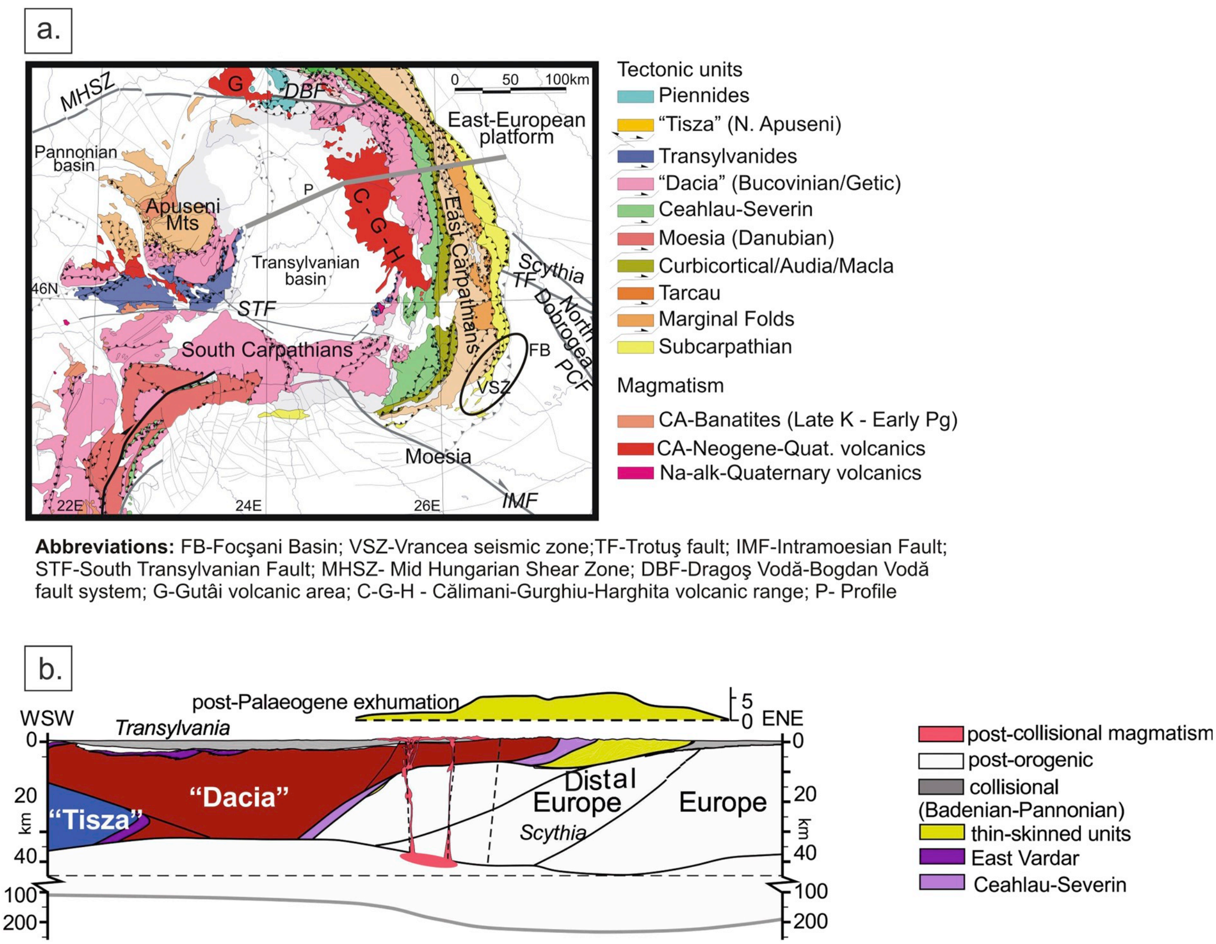


**Fig. 1.** (a) Location of the Călimani-Gurghiu-Harghita (CGH) volcanic range within the tectonic map of the Romanian Carpathians (compiled from Mațenco et al., 2010; Săndulescu, 1984; Schmid et al., 2008). (b) Interpretative cross-sections through the post-collisional environment of the CGH, including magmatic system (after Mațenco et al., 2010).

example of post-collisional volcanism. It forms a continuous volcanic zone that spreads for > 160 km along the convergent plate boundary between the East European plate and the Tisia-Dacia microplate (Figs. 1a, 2). It reflects typical post-collisional conditions postponing the subduction of an oceanic lithosphere in front of the East European plate (e.g., Mațenco, 2017 and references therein.). The CGH volcanic range rises morphologically above the eastern Transylvanian Basin and, with the exception of its southern termination (e.g., Szakács et al., 1993), it is almost parallel to the orogenic belt of the Eastern Carpathians (Fig. 1a). Its generation follows the eastward thrusting of Tisia-Dacia, which docked inside the European foreland during the Miocene (e.g., Mațenco et al., 2010 and references therein) (Fig. 1b).

Here, we wish to improve our understanding of the tectonic and structural control on post-collisional magmatism. Our work relies on tectono-structural, morphological and geophysical data (magnetic and gravimetric) integrated with eruptive outputs along the CGH range. We intend to approach the distribution and evolution of the post-collisional crustal tectonic features during the latest Miocene–Quaternary times, after nappe stacking. We examine the N-S development of tectonic structures following the mountain building process to reveal the relationship between the magmatism and volcanic activity, intra-mountain basin development and large-scale faulting characteristic to the post-collisional setting of the East Carpathians.

## 2. Geology and tectonic setting

### 2.1. Structural setting

The Carpathian fold and thrust belt is a result of the oblique docking of the Tisia–Dacia block in an upper plate position to the East European/Scythian and Moesian plates. (e.g. Ustaszewski et al., 2008; Mațenco et al., 2010). The foreland-coupling collision resulted in deformation that thickened the lower plate along steep reverse faults (Mațenco et al., 2010). The termination of outward-verging thrusting and nappe emplacement over the European foreland ended at ca. 11 Ma (Fig. 1; Mațenco and Bertotti, 2000). After collision, the plate boundaries become sealed and are closely followed by the step by step generation of the CGH chain. The deformations continue after the main collisional event, due to crustal and/or lithospheric folding (Cloetingh and Burov, 2011), thermal re-equilibration (Toussaint et al., 2004) or by erosional destruction (Sanders et al., 2002). A simplified map and a lithosphere cross-section (Fig. 1a, b) show the location where post-collisional magmatism crosses both the lower and the overriding plates. A surface uplift on the overriding plate is observed, e.g., Tisia-Dacia-Transylvanian Basin (Mațenco et al., 2010). This suggests the subduction of a buoyant continental material and its isostatic compensation (e.g., model B of Bottrill et al., 2012).

The petrological differences that develop from N to S along the CGH (e.g., Seghedi et al., 2004a) are connected to the differences in foreland rheology (i.e. the structure of the plates, their ability to react to stresses and to deform). The differences occur between the northern part (East

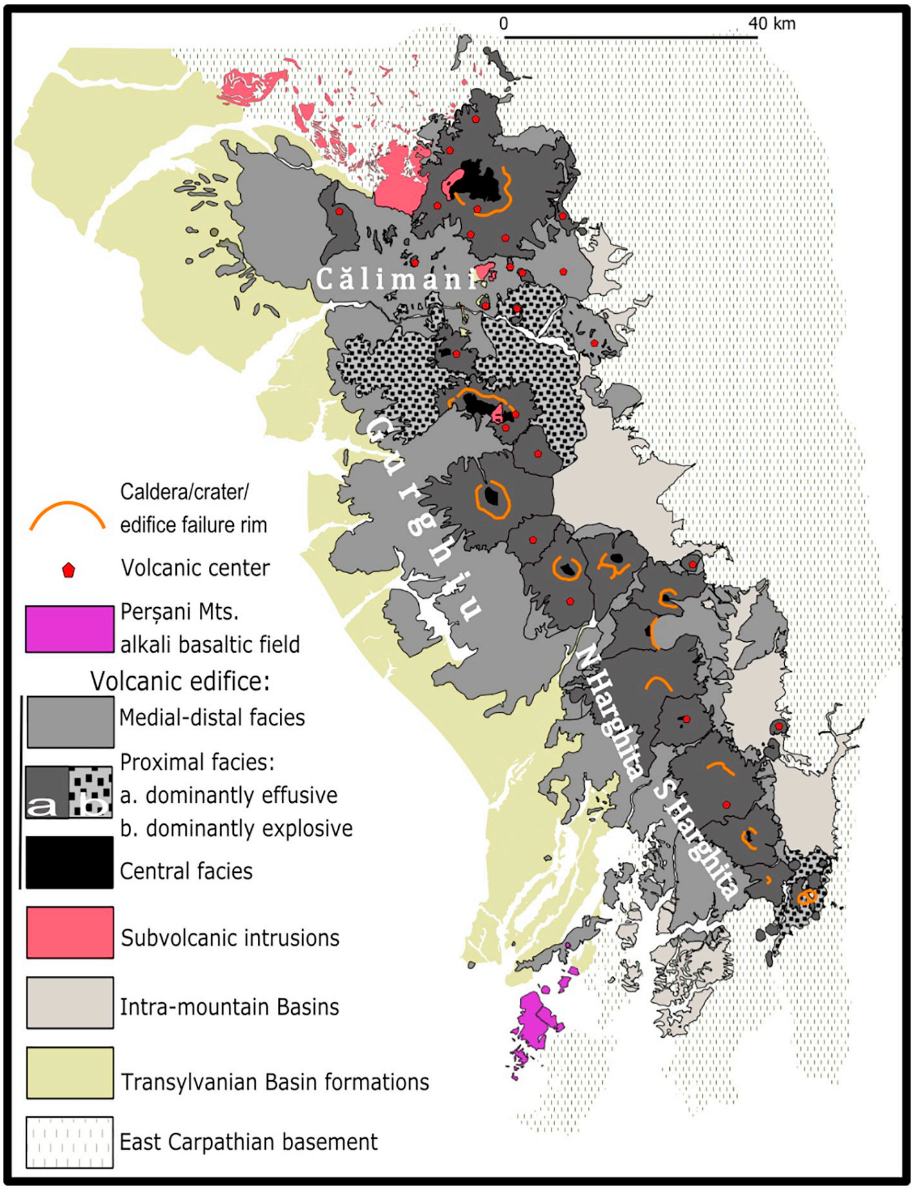


**Fig. 2.** Simplified volcanic facies map of the Călimani-Gurghiu-Harghita volcanic range (modified from Szakács and Seghedi, 1995).

European and Scythian plates) and the southern part (Moesian plate) (Cloetingh et al., 2004 and references therein), separated by the Trotuş fault. For example, in the north, the collision was oblique, being accommodated by orogenic exhumation in the order of 6 km (Gröger et al., 2008). This affected the petrology of the magmas that suggest subcontinental mantle heterogeneities in the source areas, and by promoting crustal anatexis via decompression melting (Fedele et al., 2016). Towards the south, the collision was associated with a reduced uplift (Sanders et al., 1999) and a subsidence in the foreland, with an amplitude of up to 6 km (Tărăpoancă et al., 2003). This affected the petrology of the magmas by generating normal calc-alkaline melts in front of European/Scythian plate (> 4 Ma) and by generating adakite-like calc-alkaline, mafic Na-alkalic and shoshonitic K-alkalic melts in front of the Moesian plate (2.8–0.03 Ma) (Seghedi et al., 2011). It was proposed that the CGH volcanic range and the intra-mountain basins are part of the same tectonic structure. This is a regional post-collisional NNW–SSE striking sinistral transtensional zone (Fielitz and Seghedi, 2005). The fault zone system allowed the formation of magma pathways to the surface. These pathways allowed the ascent of magmas from the upper mantle sources and from the lower crustal magma chambers (Mason et al., 1995, 1996; Seghedi et al., 2004a).

### 2.2. Volcanism and intra-mountain basins in the inner Eastern Carpathians

The CGH is situated to the east of the Transylvanian Basin. The volcanic edifices rest unconformable to the east and southeast, on several Inner Carpathian nappes, while to the west and southwest they overlie the Late Miocene sediments of the Transylvanian Basin (Szakács and Seghedi, 1995).

The CGH volcanic range is associated with a series of tectonic basins. These are the Bilbor/Borsec-Gheorgheni-Ciuc intra-mountain basin system (e.g., Săndulescu, 1984) and the Braşov basin system to the south (Fig. 3a, b). The basin fill is dominated by fluvial-lacustrine clastic deposits and coal, including important volcano-sedimentary deposits derived from the CGH volcanic edifices.

The southernmost evolution of the Pliocene–Quaternary Braşov Basin system is a result of post-collisional stresses. These are related to the rise of the asthenospheric mantle in the hinterland of the rapidly sinking Vrancea slab, as inferred by a wide array of deep geophysical observations and numerical modeling (Ismail-Zadeh et al., 2012 and

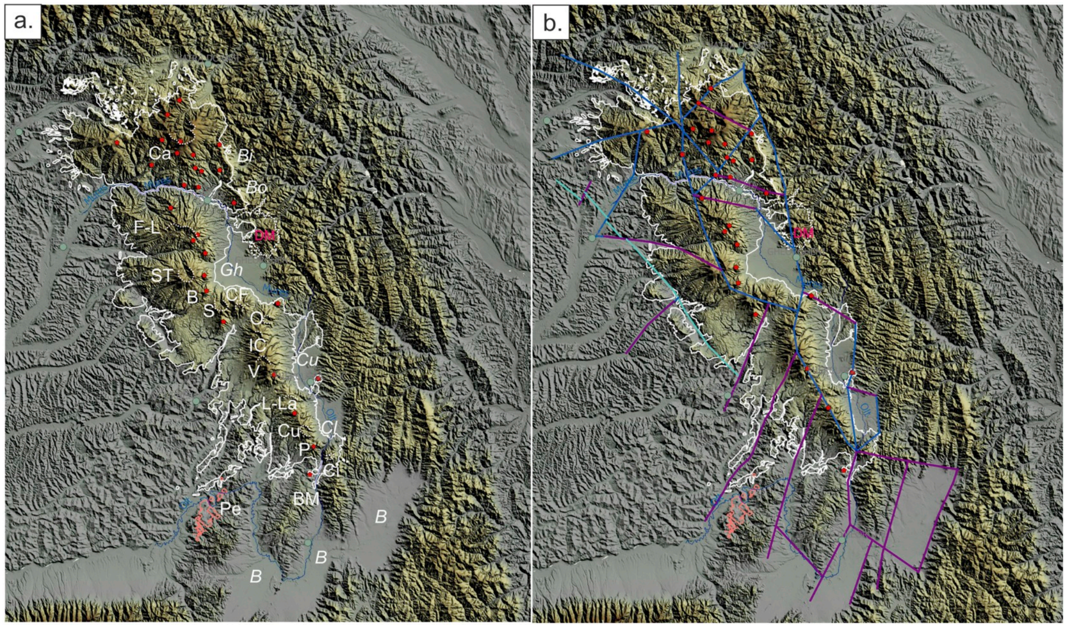


**Fig. 3.** (a) Morphological map of the CGH: Ca, Călimani; F-L, Fâncel-Lăpuşna; ST, Seaca-Tătarca; B, Borzont; S, Şumuleu; CF, Ciumani-Fierăstraie; O, Ostoroş; IC, Ivo-Cocoizaş; V, Vârghiş; L, Luci-Lazu; Cu, Cucu; P, Pilişca; Ci, Ciomadul and Pe, Perşani basaltic volcanic field; intra-mountain sedimentary basins: Bi, Bilbor; Bo, Borsec; Gh, Gheorgheni; UC, Upper Ciuc; LC, Lower Ciuc; B, Braşov; Ba, Baraolt; DM - Ditrau syenite Massive; (b) Tectonic features of the CGH (compiled after Seghedi et al., 1994; Fielitz and Seghedi, 2005; Krézsek and Bally, 2006; Szakács and Krezsék, 2006). The fault represented in light blue is associated with salt diapirs; deep blue color corresponds to strike slip faults; violet corresponds to normal faults. (For interpretation of the references to color in this figure legend, the reader is referred to the web version of this article.)

references therein).

Previous studies reveal the dominant subalkaline composition of the CGH volcanic range (Seghedi and Downes, 2011 and reference therein). The subalkaline magmas generated various types of chain-like volcanic structures: calderas, composite volcanoes, lava domes, etc. The ages become progressively younger towards the south (from 10 to 0.03 Ma) and the erupted volumes become smaller (Fig. 2). The oldest rocks are in the NNW, in the Călimani Mts. (Pécskay et al., 2006), while the youngest are in the SSE, at Ciomadul volcano (e.g., Szakács et al., 2015; Molnár et al., 2019). The spatial and temporal distribution of the volcanism (Pécskay et al., 2006 and reference therein) was tectonically controlled (e.g., Mason et al., 1998; Seghedi et al., 1998; Szakács and Krezsék, 2006).

The volcanic edifices are mostly composite volcanoes. The volcanic structures partially overlap and are mainly andesitic in composition. Two volcanic edifices in the Călimani and northern Gurghiu Mts. reached caldera stages that have been followed by the extrusion of dome complexes, including summit and peripheral domes (Szakács and Seghedi, 1995). Edifice failure and related debris avalanche deposits occurred at several composite volcanoes (e.g., Szakács and Seghedi, 2000). Debris avalanche deposits dominate the western part of the CGH.

In the post-collisional context of the CGH, magma generation is not contemporaneous with the dehydration of the slab, nor with the ascent of fluids into the asthenospheric wedge between the upper and lower plates. In other words, it is not related to the development of a melting front above the slab, as is typical in subduction processes. Instead, the magma generation processes are connected to post-collisional lithosphere melting at the mantle-crust boundary; this occurs during asthenospheric upwelling, after slab breakoff (e.g., Seghedi and Downes, 2011 and reference therein) (e.g., Fig. 1a, b). This is supported by the present high heat flow matching the volcanic area (Tari et al., 1999; Demetrescu et al., 2001).

## 3. Methodology

The case study area is investigated by (i) integrated GIS mapping, (ii) geophysical gravity and (iii) geophysical magnetic mapping. The data was acquired by the INSTEC team during 2014–2016. The three resulting datasets are integrated with previously published data to provide a comprehensive overview of the post-collisional magmatic features of the CGH.

(i) The Open Source QGIS software (qgis.org) is used to integrate tectonic, structural, morphologic and geophysical data. The morphology of the CGH is generated from the Shuttle Radar Topography Mission (SRTM) datasets with a resolution of 3 arc sec. The tectonic data is taken from the most recent work dealing with the tectonic features of the CGH (Fielitz and Seghedi, 2005). We use the main fault patterns and main volcanic structures to generate a landmark system that we use on all the maps. Faults and other tectonic elements form linear geomorphology (linear structures on the topographic surface). These linear structures control the distribution of regional geological formations, including aquifers, geothermal systems, volcanic edifices and magmatic intrusions. The linear tectonic features indicate the strength and stability of the geological structure that was exposed to multiple tectonic deformations. A simple visual analysis reveals two kinds of linear structures: (1) those affecting the basement, which are easy to observe on a regional scale and (2) those related to the linear distribution of the volcanic edifices and large subvolcanic intrusive bodies. Volcanic edifice volume calculations are based on combining geological maps with 1:25000 scale Digital Elevation Models generated from the SRTM dataset.

(ii) Gravity measurements were done by the INSTEC team with a Scintrex CG-5 AUTOGRAV meter calibrated at the start of the field campaign on the UNIGRACE calibration line in Cluj-Napoca – Beliș (172.12 mgal). The potential instrumental drift was checked for regularly in the underground gravity lab of the Solid Earth Dynamic Department of the Institute of Geodynamics of the Romanian

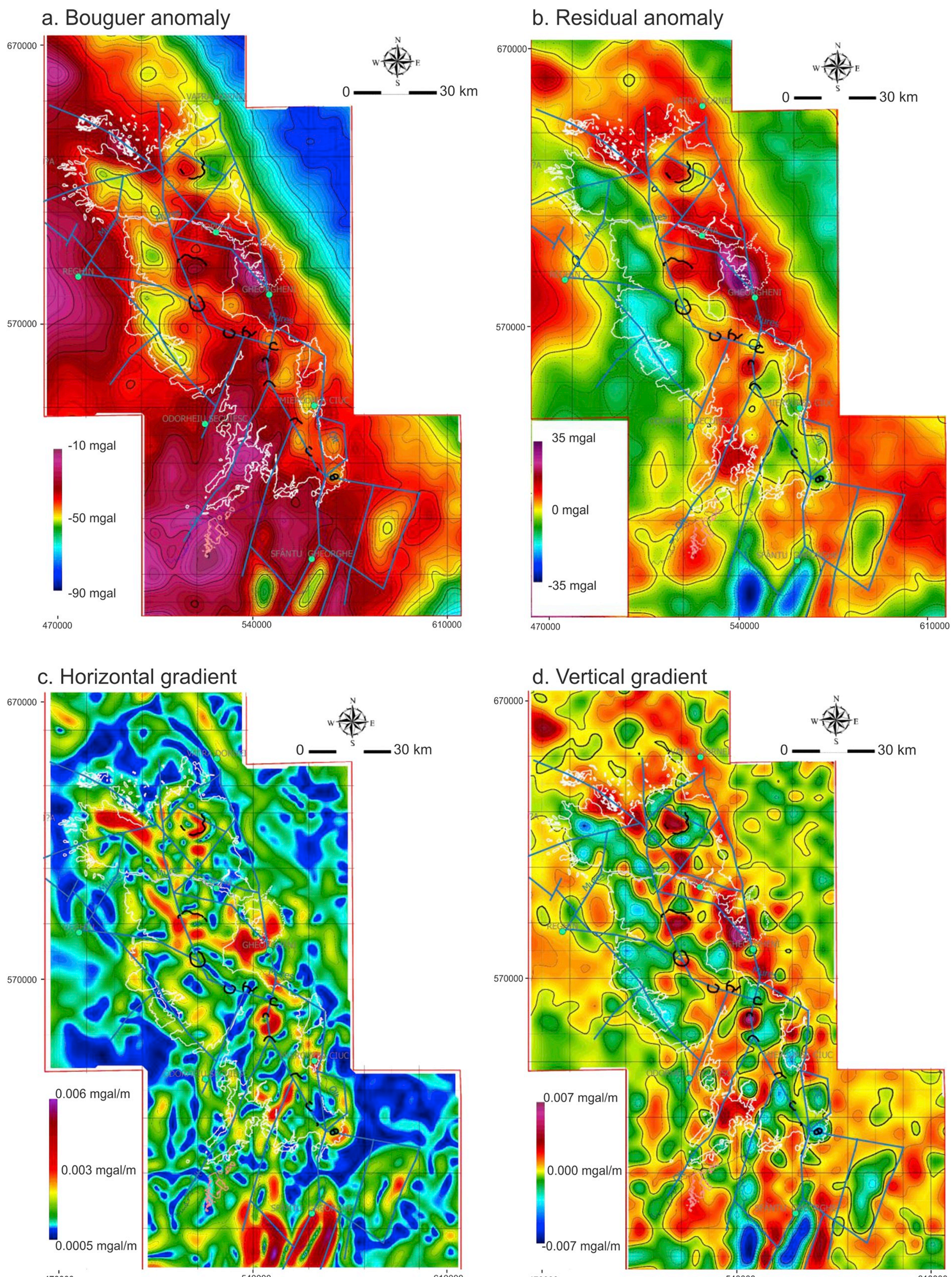


**Fig. 4.** Geophysical gravity maps: (a) Bouguer anomaly, (b) residual gravity anomaly, (c) horizontal gradient of the residual gravity anomaly, (d) vertical gradient of the residual gravity anomaly. Bouguer correction radius is 20 km, Krigging interpolator with cell size of 5 × 5 km, DTM map scale 1:100000, projection system Stereo 1970, altitude datum Black Sea 1975.

Academy. Absolute gravity transfer has been achieved by designing and implementing special reference networks providing gravity ties to base stations belonging to the Romanian national gravity system or to the European UNIGRACE network. Gravity observations have been performed within repeated measuring cycles based on several local base stations of the survey (e.g. Milsom and Eriksen, 2011; Hinze et al., 2013). Local reference stations were located in the neighborhood of the Lepşa and Topliţa base stations belonging to the second order national reference network.

The primary processing of gravity data aims at providing data consistency. The following corrections have been applied (e.g. Hinze et al., 2013): instrumental reductions (tidal effect and residual drift), base reduction and computing the absolute gravity value, theoretical gravity (latitude) reduction (Silva, 1986), elevation reduction, Bouguer plate reduction, Bouguer correction. Therefore, the Bouguer anomaly is calculated for each measurement point based on the two standard density values formally used in the National Gravity Map of Romania: 2200 $kg/m^3$ and 2670 $kg/m^3$. Both values may be equally employed, but the higher density performs better at eliminating the topographic effect and is therefore used hence-forth.

(iii) Magnetic measurements were performed by the INSTEC team with a Geometrics G856 AX proton magnetometer used as a mobile field station and with a Scintrex SM-5 NAVMG optical pump magnetometer used as a base station to account for the diurnal activity/shifts in the ambient magnetic field. The new dataset has been integrated with the geomagnetic data from the national database (e.g., Airinei et al., 1969). Data processing involves diurnal activity correction and base reduction (e.g. Reeves, 1995; Milsom and Eriksen, 2011). The anomaly of the total magnetic field intensity has been computed by subtracting the reference geomagnetic field from the acquired data (e.g., Reeves, 1995; Hinze et al., 2013). The IGRF 12 model (Erwan et al., 2015) was applied to remove the planetary effect.

## 4. Results

### 4.1. Development of tectonic basins and volcanic activity

The lineaments' distribution of the Călimani and northern Gurghiu volcanic mountains is closely associated to the evolution of Late Miocene (10.5–6.5 Ma) volcanic centers (e.g., Szakács and Seghedi, 1996). For example, a linear distribution of subvolcanic intrusions precedes and is coeval with the active volcanic activity along a NW-SE direction (~10–9.5 Ma) (Figs. 2 and 3a, b).

The main structural and tectonic feature of the CGH is the association of volcanic edifices with intra-mountain basins (Fig. 3a, b). Four major graben-like structures are observed to have developed from N-S, bounded by oblique sinistral faults with a normal dip component. The four graben structures are pull-apart basins developed in the transfer areas of a NNW-SSE striking transtensional fault zone with left stepping stepovers and pull-apart basins in the transfer areas (a fault stepover forms when individual segments of the fault overlap and link together) (Figs. 6 and 7). These tectonic structures have formed on the previously thrusted nappes belonging to Tisia-Dacia. The northernmost basin is the least developed, while the other basins have deeper footwalls. The infills of these basins are estimated at 200 m thickness, and 800–1000 m, respectively (Fielitz and Seghedi, 2005 and references therein).

The eruptive centers have mostly developed either inside the basins or along the main fault-zones bounding them. From a total of 27 vents, 17 (62%) coincide with the main basin-delimiting fault zones, 7 (27%) have emerged well within the basins and only 3 (11%) have developed outside, but in the proximity of secondary adjustment/transfer faults. Most of the volcanic edifices are concentrated on the western side of the tectonic structure, with only 5 that have developed on the eastern edge.

Another interesting feature of the western flank of the CGH is the proximity to an important NW-SE fault system. This is crosscut by the faults of the CGH and intra-mountain basins. The associated salt diapiric formations suggest that this older tectonic feature represents a major fault zone (Krézsek and Bally, 2006).

The southern tip of the main pull-apart basin-system connects to the younger Braşov basins. Here, Pleistocene Na-alkalic basaltic volcanism has taken place (Seghedi et al., 2016) (Fig. 3a, b). The contemporaneous nature of the CGH volcanism with intra-mountain basin development is evident from the nature of the infilling basin sediments. Volcaniclastic deposits, both primary and secondary (reworked pyroclastics, debris avalanche deposits, etc.) are associated with fluvial-lacustrine clastic sediments. The coeval ages are also confirmed by the sediment paleontological data and K/Ar volcanic ages (Fielitz and Seghedi, 2005 and references therein; Pécskay et al., 1995).

### 4.2. Geophysical insights: gravity data

The Bouguer anomaly and the residual gravity map show a number of similarities that reflect the gravity effects of large scale structures (Fig. 4). These dominate the Bouguer anomaly map and are retained in the background gravity signal of the residual map. They suggest thick geological bodies extending to depth all the way from, or near the surface. For example:

1. The strong negative anomaly eastwards of the CGH corresponds to the folded and thickened crust of the Carpathian Orogen. It reflects the low density of sedimentary deposits;
2. The area corresponding to the northern and central parts of the CGH and intra-mountain basin systems (Călimani and Gurghiu Mts.) reflects low Bouguer values and positive residual anomalies. The two types of anomalies are in perfect accordance. This reflects the presence of high-density geological structures (potentially subvolcanic intrusions). These extend relatively close to the surface and overprint the negative anomaly that would normally be associated to the low-density sediments filling the basins: hence, the positive anomalies on the residual gravity map;
3. The southern intra-mountain basins associated to the CGH (Harghita Mts.) show negative residual magnetic anomalies which correlate to low Bouguer values. These indicate a dominant effect of low-density sediments and the scarcity of volcanic intrusions in this segment of the CGH (which must be of small-volume, anyway);
4. The central-eastern side of the CGH shows positive residual anomalies and high Bouguer values. The anomalies are associated with the Ditrău syenite massif (which is part of the basement). The syenite structure seems to extend to depths large enough to generate a regional gravity anomaly;
5. The Braşov Basins towards the SE of the CGH show negative anomalies. This suggests relatively deep tectonic structures filled with sediments;
6. Local positive residual anomalies and high Bouguer values are observed towards the W and SW of the CGH. The anomalies reflect high-density geological bodies extending close to the surface (potentially magmatic intrusions);
7. Negative residual anomalies and low Bouguer values are observed directly westward of the CGH. These partly correspond to the older fault-zone discussed earlier and potentially indicate an older, infilled tectonic basin.

On the other hand, the Bouguer and residual gravity maps show a major difference related to the nearby Transylvanian Basin. The residual map highlights a predominant negative gravity anomaly that contrasts with the high Bouguer values. This suggests the presence of deeply buried high-density geological formations covered by low-density rocks.

The horizontal residual gravity gradient map highlights density changes in the shallow environment, mostly related to tectonic features (Fig. 4). The positive anomalies bordering the western edge of the CGH mark the contact of the volcanic range with the older basin-feature described at point 7. Similarly, the positive anomalies from the Brașov Basins towards the south of the map emphasize the horst features delineating the extensional basins. A number of these geophysical limits albeit less contrasting, are observed on the eastern edge of the CGH. They mark the boundaries of the intra-mountain basins. Interesting exceptions are the positive anomalies recorded within the CGH, which indicate shallow magmatic bodies (subvolcanic intrusions) or extensive effusive deposits, the most visible corresponding to the Ditrău Massif (Fig. 3a, b). Generally, these types of anomalies are larger in the northern part of the CGH and diminish in size towards the south. This indicates less extensive intrusions towards the south: a perfect link can be drawn to the surface geological data showing smaller eruptive volumes and less complex volcanoes.

The vertical residual gravity gradient map highlights vertical density changes in the shallow environment, mostly related to magmatic features (Fig. 4). This map is particularly useful for identifying subvolcanic intrusions. Unsurprisingly, most of the positive anomalies are located within the CGH and associated intra-mountain basins. A key observation is that virtually all of these subvolcanic bodies have developed along or at the intersection of faults.

### *4.3. Geophysical insights: magnetic data*

The total magnetic intensity and residual magnetic anomaly maps are very similar. This suggests that the high magnetic susceptibility bodies generating the anomalies are located in the shallow geological environment and potentially extend to greater depth (Fig. 5). The positive anomalies are mostly located within the CGH, and they partly coincide with known fault zones. As with points 2 and 3 of the gravity data, the largest and more intense magnetic anomalies are located in the northern and central parts of the CGH. These also diminish in size and intensity towards the south. An important anomaly coincides to the Ditrău massif, but the largest positive magnetic anomaly coincides with the Gurghiu segment of the CGH.

The horizontal gradient of the reduced-to-pole residual magnetic anomaly highlights the limits of the effusive and potentially intrusive subvolcanic bodies (Fig. 5). The anomalies overprint most of the intra-mountain basins and are more extensive than the gravity anomalies. They might reflect a combined signal of the denser effusive and intrusive magmatic rocks with the magnetic signal of the less dense pyroclastic deposits. In concordance to the gravity gradient maps, it suggests that (i) the volcanoes and shallow intrusions are concentrated along faults and at fault intersections and (ii) magmatic features are larger in the northern and central parts of the CGH and less developed towards the south. In addition, an isolated positive residual magnetic anomaly is identified northeastwards of the CGH. It has no correspondence in the gravity maps. Another interesting feature is a linear NNW-SSE positive anomaly recorded in the Transylvanian basin, quasi-parallel to the CGH.

The vertical gradient of the reduced-to-pole residual magnetic anomaly indicates the presence of five high magnetic susceptibility geological structures in the northern side of the CGH (Fig. 5). These underlie the Ditrău Massif and Călimani and Gurghiu volcanoes. Their locations coincide with the projection of the main vents/craters/calderas. The apparent diameter of these anomalies is at least five times less than the diameter of their counterparts from the horizontal gradient map. The anomalies mark the location of the main plumbing systems feeding the subvolcanic intrusions and the eruption centers.

### *4.4. Volumes of erupted magma along the CGH*

The volume of erupted magma, including eruptive rates along the CGH, have been evaluated by Szakács et al. (1997) and Karátson and Timár (2005). Here we provide our re-evaluation of the data, in the light of recent studies (Seghedi et al., 2017) (Table 1). CGH is divided into five segments. The division is based on differences in the strikes and positions of volcanic lineaments and on the time intervals when the volcanic range was active. We took into consideration the volume displaced by erosion, which is estimated at 30 m/Ma, in accord with the estimations of Karátson and Timár (2005). The volumes of erupted magmas are similar with the volumes erupted by typical “arc volcanoes” (e.g., Acocella, 2014). The South Gurghiu area has the highest output rates, while the South Harghita segment has the least voluminous extrusions.

## 5. Discussion

### *5.1. A review of tectonic and magmatic development in the light of structural data*

The spatial distribution of the volcanic centers corresponds to NNW-SSE and NE-SW trending systems. The NW-SE striking fault zone corresponds to the volcanic centers that were active between 10.5 and 9.5 Ma (Bârgău Mts.) and the NE-SW faults mark the eruptive centers active between 9.5 and 8 Ma (Călimani Mts.) (Szakács and Seghedi, 1996). The volcanic activity along these faults is partly synchronous and is progressively replaced by activity taking place along a southerly located NNW-SSE fracture system. This happens between 8 and 6.5 Ma. From 6.5 to 0.03 Ma volcanism migrates towards the SSE, paralleling the Gheorgheni - Ciuc basins. Structural observations confirm the normal and strike-slip fault systems associated with the intra-mountain basins and CGH. The main displacement trends along strike-slip and normal faults are shown in Fig. 6.

Our interpretation agrees with the model presented by Fielitz and Seghedi (2005). It confirms the simultaneous intra-mountain basin and magmatism generation during Miocene-Quaternary in the CGH (between 10 and 5.5 Ma in the **N** and between 5.5 and 0.03 Ma in the S) (Fig. 7). One important argument is that the sinistral basin-bounding faults control the location of volcanic centers and the orientation of the feeder dikes. We argue that the slight changes in the trending orientation of the volcanic range are in close relation to fault and basin development. Therefore, they are in close relation to local stress fields, basement cohesion-fragmentation and potentially to the geometry of the contact between the adjacent East European/Scythian and Moesian plates. This latter point can be argued based on the slight orientation change of the volcanic range and intra-mountain basins. The orientation changes from NW-SE and WNW-ESE (in the northern CGH) to NNW-SSE. This happens as the basins develop in the proximity of the contact in question, at the Carpathian Bend Area. The inflection point corresponds to the contact of the intra-mountain basins with the Trotuș Fault, depicted in Fig. 6. The Trotuș fault is the main boundary between the East European/Scythian and Moesian plates, marking the southern step-back of the Moesian margin (Mațenco et al., 1997). The Trotuş fault marks a strong contrast in lithosphere geometry (thickness, shape, etc.). This is well expressed in the Bouguer gravity anomaly by the clear offset at the transition between the East European/Scythian and Moesian platforms (Cloetingh et al., 2004). Also, the Subcarpathian nappe is thrust over the foreland to the north of the Trotuș fault. To the south, the Carpathians front is outlined by a recumbent fold, which is overlain by Upper Sarmatian-Quaternary sediments (e.g., Săndulescu, 1984). The effect that this tectonic contact has on the development of the CGH magmatism and intra-mountain basins is an argument for the oblique collision with Tisia-Dacia: if the collisional front changed its orientation due to the pre-existing geometry of the Carpathian embayment, the resulting stress fields also changed the orientation of the mountain-basins and volcanic range. This has also been suggested by Mason et al. (1998) and coincides with the South Harghita segment of the CGH crossing the collided accretionary prism system towards the south (Szakács et al., 1993). According to the K-Ar volcanic ages, the

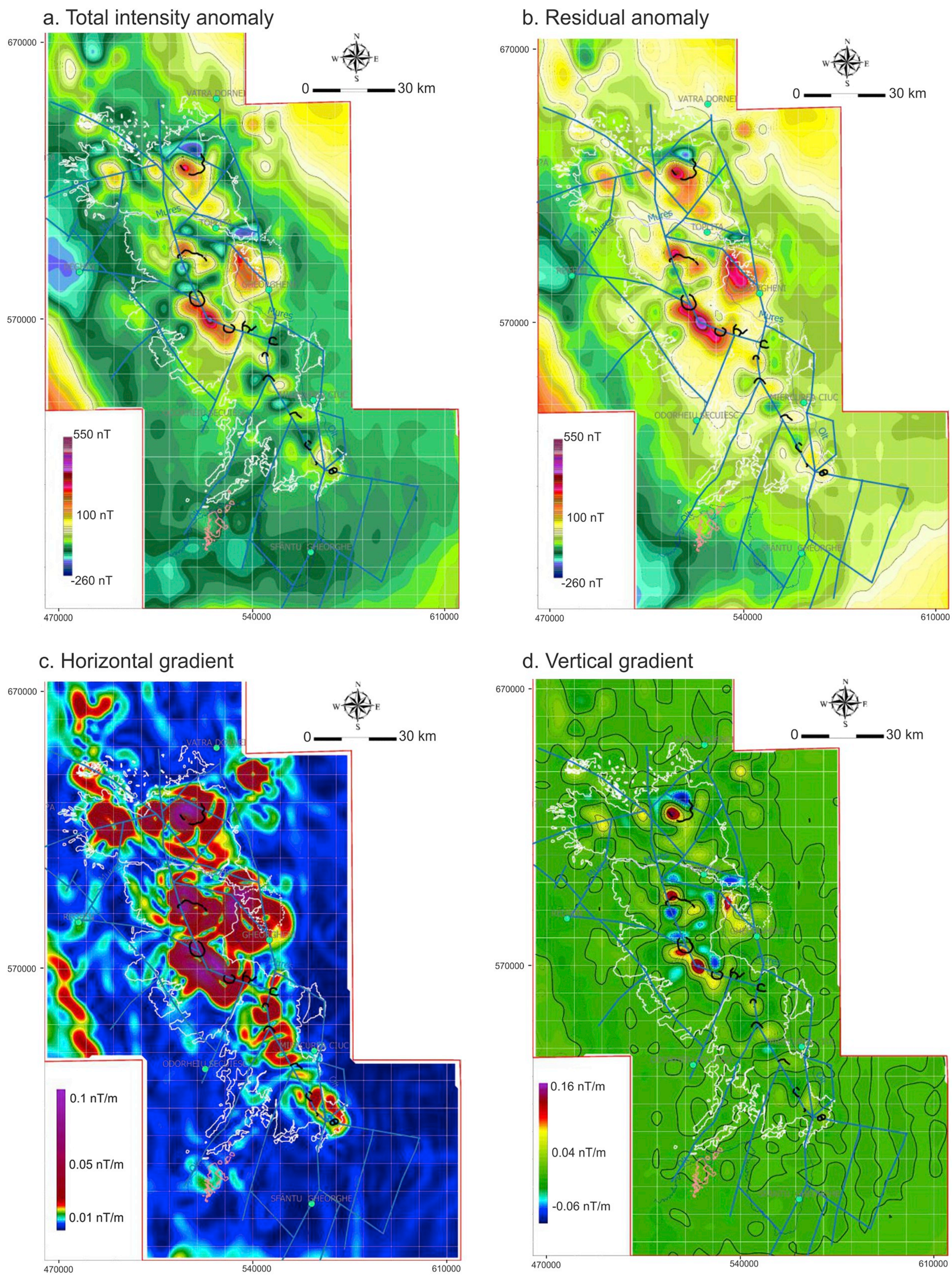


**Fig. 5.** Geophysical magnetic maps: (a) Total intensity anomaly, (b) residual magnetic anomaly, (c) horizontal gradient of the residual magnetic anomaly, (d) vertical gradient of the residual magnetic anomaly. Geomagnetic reference field IGRF12, reference altitude 2500 m, Kriging interpolator with cell size of 5 × 5 km, DTM map scale 1:100000, projection system Stereo 1970, altitude datum Black Sea 1975.

**Table 1**
Erupted volume include also an estimated eroded volume calculated with parameters estimated for CGH according to Karátson and Timár, 2005.

| Segment | Volume ($km^3$) | Migration rate (km/Ma) | General output rate ($km^3$/Ma) | Per km output rate ($km^3$/Ma/km) | R $km^3$/yr/100 km segment |
|---|---|---|---|---|---|
| Călimani | 784.4 | 17.6 | 230.7 | 3.8 | $3.8 \times x\ 10^{-4}$ |
| North Gurghiu | 284.2 | 10.7 | 101.5 | 3.4 | $3.4 \times 10^{-4}$ |
| South Gurghiu | 210.8 | 33.3 | 175.7 | 4.4 | $4.4 \times 10^{-4}$ |
| North Harghita | 206.9 | 14.6 | 86.2 | 2.5 | $2.5 \times 10^{-4}$ |
| South Harghita | 120 | 7.7 | 26.7 | 0.8 | $0.77 \times 10^{-4}$ |

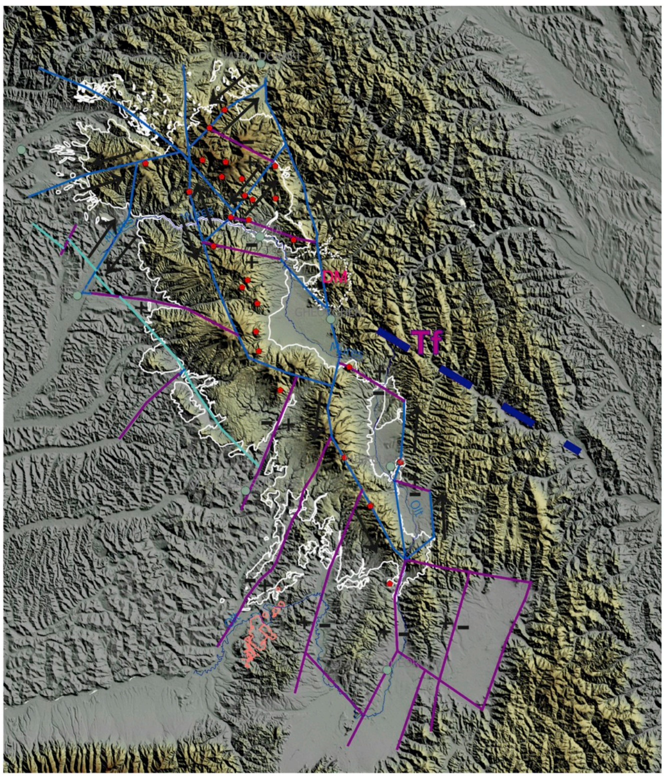


**Fig. 6.** The configuration of normal and transcurrent faults and fractures. It governed the evolution of Late Miocene–Quaternary volcanism and basin subsidence along a transtensional corridor in the CGH range. The volcanic centers are concentrated along the western margin of this corridor (modified after Fielitz and Seghedi, 2005). All the details and signs are the same as those explained in Fig. 3a, b.

inflection of the CGH and intra-mountain basins took place effectively at around 6.5–5.5 Ma (Pécskay et al., 2006; Seghedi et al., 2004b). It is important to note that between 6 and 5 Ma, the source of the Upper Miocene to Pliocene deposits from the nearby outer-Carpathian basins changes (i.e. Focșani basin towards the SE of the Carpathian Bend Area). The change is from a dominantly volcanic source (Călimani-Gurghiu area), to a recycled orogenic belt source with increasing accumulation rates suggesting exhumation and erosion of the East Carpathian napes (Panaiotu et al., 2007). Additionally, this coincides with the volcanic activity moving towards the southern segment of the CGH, where the extruded volumes are also reduced. Hence, they provide a reduced amount of volcanic source-material for sedimentary basins. The dominant tectonic evolution of the CGH area and associated basins is marked by dominant horizontal and vertical movements. This is confirmed by paleomagnetic surveys that rule out any major block rotations during magmatic emplacement (Panaiotu et al., 2012; Vişan et al., 2016).

### 5.2. Tectonic and magmatic features revealed through geophysics

The gravity and magnetic surveys separate the investigated region in four main areas with distinct geophysical properties:

1) **The Eastern Carpathian orogen** to the east, where the geophysical data indicates crustal thickening by accretion of low-density sediments. This area is generally free of magnetic anomalies, with the exception of the NE feature well-defined in the gradient maps of the residual magnetic anomaly. This is potentially a subvolcanic low-density intrusion isolated from the CGH;

2) **The CGH volcanic range** associated with the intra-mountain basins, which is the most geologically and geophysically contrasting feature of the investigated area. The geophysical data indicates distinct and sharp tectonic boundaries between the basins and nearby mountains. This supports the earlier interpretations of deep pull-apart structures. The magmatic features, including effusive units and subvolcanic intrusions are concentrated on the main tectonic features, but preponderantly along the western margin of the CGH. Here, the basin-forming faults are in the proximity of an older tectonic feature. This older feature is associated with a deep, infilled paleo-basin and indicates a fragmented basement. The coincidental conjunction of these tectonic structures creates a zone of least-resistance. This zone allows the permeation of magma and the development of ascent paths, plumbing systems and an array of magmatic intrusions that feed the post-collisional volcanic activity of the CGH. This explains the preferential emplacement of the volcanic edifices on the western side of the intra-mountain basins. In addition, the plumbing system coinciding to the Gurghiu segment (western side of the basins) has a strong geophysical signal. It potentially marks the most extensive plumbing system of the CGH. With all these in mind, considering the geological profile from Fig. 1, this indicates that magmatism penetrated the margin of the underlying tectonic plate (Scythian segment of the East European Platform) and also the overlying thrusted margins of the Tisia-Dacia plate. This situation is representative for post-collisional magmatism and distinct from classical subduction systems where the magmatic structures are generated exclusively in the overriding plate, before thrusting takes place (e.g., Seghedi and Downes, 2011).

Another important observation is the geophysical separation of the CGH in two distinct areas.

(i) One of the areas is represented by the northern and central parts of the CGH, with well defined, large and intense gravity and magnetic anomalies. These suggest the development of extensive magmatic features, both in the shallow and deep environment. The shallow geological environment of the basin infill seems to be dominated by strong geophysical signatures, suggesting large volcanic output rates. Here, the northwestern-most anomalies reveal the NW-SE linear development of intrusive subvolcanic bodies. These extend from the Rodna-Bârgău Mts., outward in respect to the CGH.

(ii) The second area is represented by the southern part of the CGH, where the basins become narrower (south of the Trotuș Fault). The magnetic and gravity anomalies, both in the shallow and deep environment are minor in comparison to the northern segment. This indicates less significant magmatic structures and correlates well with the reduced sizes and complexities of the volcanic edifices. The geophysical signal of the basin infills is also reduced. Hence, it indicates a smaller volcanic output (Table 1) and a larger proportion of sedimentary source materials. This correlates with volumetric volcanological information (e.g., Szakács et al., 1997; Karátson and Timár, 2005). Basically, the change in the geophysical nature of CGH corresponds to the change in its structural orientation. This was also mentioned in the previous section: the inflection in the proximity of the Trotuș Fault. The observation supports the asymmetric convergence and oblique collision of the Tisia-Dacia

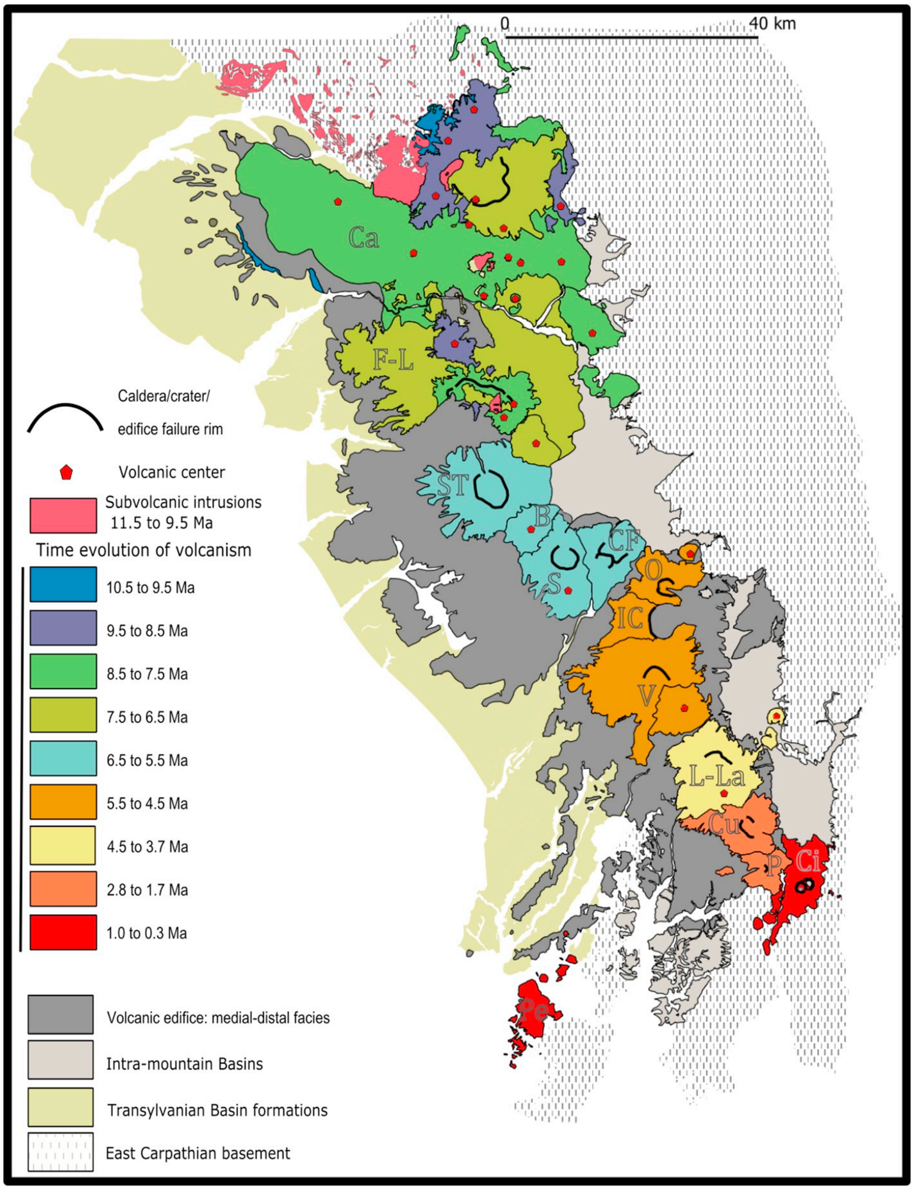


**Fig. 7.** The evolution in space and time of the main composite volcanoes along the CGH range (age data after Pécskay et al., 1995, 2006; Molnár et al., 2019). Name abbreviation of the volcanoes as in the Fig. 3a.

block with the East European platform.

3) **The Brașov extensional basins** to the south of the CGH. The geophysical data outlines well defined NE-SW graben-horst features that connect to the southernmost tip of the post-collisional magmatic range. The two tectonic provinces have at least one stage of coeval development. This is indicated by the extension of the CGH magmatism towards the eastern Brașov basins.

4) **The Transylvanian basin** with its strong deep gravity anomalies. The lack of any associated magnetic anomaly can be explained by the intense loss of magnetic signal with depth. This suggests a deep environment for the geological feature inducing the high gravity anomaly. This can be related to the deeply buried basement of the Transylvanian basin or to an array of deep magmatic intrusions. The magmatic intrusions scenario is supported by two observations. For example, it is supported by (i) the presence of isolated shallow positive gravity anomalies (i.e. residual gravity map) that could indicate upward extensions of these presumed intrusions. Also, it is supported by (ii) the linear feature with a strong positive magnetic anomaly seen in the shallow environment of the Transylvanian basin (i.e. horizontal gradient magnetic map). This could mark the location of a dyke system developed quasi-parallel to the CGH.

### 5.3. Post-collisional volcanic range and back-arc controversy

The post-collisional setting of the CGH is confirmed by:

- (i) the generation of magmatism and volcanism after nappe stacking (collision);
- (ii) the progressive younging of activity towards the south, parallel to the collisional front and to the orogen (and not quasi-perpendicular to it);
- (iii) the close structural relation between the oblique collision of Tisia-Dacia and the inflection recorded by intra-mountain basins and magmatism.

The CGH represents a typical post-collisional range. It evolved progressively from north to south in response to the brittle fragmentation of the overriding Tisia-Dacia nappes and of the underlying tip of the European Platform (Scythian segment). The fragmentation accommodated magma transport and storage in the crust (Fig. 1).

Even so, the terms “arc” and “back-arc” are controversial in the Carpathian realm, because the CHG is linear. For example, the CGH volcanic assemblage is interpreted by some authors as “arc” magmatism (e.g., Horváth et al., 2015; Maţenco, 2017 and references therein) and by other authors as “post-collisional” magmatism (e.g., Harangi et al., 2006; Seghedi and Downes, 2011). In addition, the arcuate shape of the Carpathian orogen was assimilated to that of an “arc”, inducing misunderstandings in the geological literature. In this specific case, the term “arc” simply refers to the shape inherited from the pre-collisional arcuate geometry of the landlocked basin described by the East European and Moesian plates (e.g., Ustaszewski et al., 2008).

Similarly, the Transylvanian and Pannonian Basins are sometimes referred to as “back-arc” basins (e.g., Horváth et al., 2015; Maţenco et al., 2010; Maţenco and Radivojević, 2012). However, it has been recognized that the positions of these basins behind a “magmatic arc” are unclear (Balázs et al., 2016; Maţenco, 2017). The controversy can be extended to the entire Carpathian-Mediterranean region. Here, many “back-arcs” were defined in the hinterlands of the highly arcuate Hellenides, Rif-Betics, Apennines, and Carpathians orogens. These “arcs” are assumed to have formed in relation to the Oligocene-Miocene subduction retreat of the Aegean, Gibraltar, Calabrian or Vrancea Slabs (Royden, 1993; Okay et al., 1994; Faccenna et al., 2005; Doglioni et al., 2007; Wortel and Spakman, 2000; Horváth et al., 2015; Jolivet and Brun, 2010; Jolivet et al., 2013; Vergés and Fernàndez, 2012). Although there are some similarities with typical back-arc basins from the circum-Pacific area (e.g., Uyeda and Kanamori, 1979; Heuret and Lallemand, 2005) there is not a perfect match. For example, their position is not behind a “typical magmatic arc”. The debate over the “arc” or “post-collisional” nature of many magmatic systems in the Carpathian-Mediterranean region can be elucidated by providing data and interpretation on the coeval magmatic, tectonic and basin sedimentation processes. Numerical modeling of analogous situations would be, as well, useful (e.g., Bottrill et al., 2012).

## 6. Conclusions

The geological and geophysical data of the post-collisional CGH range validates the contemporaneous formation of basins and volcanic activity. It supports the southward propagation of strike-slip and normal faulting, following the post-subduction collisional events. (e.g., Pécskay et al., 1995, 2006). It also highlights how the distribution of tectonic stresses and how the mechanisms of magma generation change as the maximum collision migrates from the East European plate, to the Moesian plate.

The CGH magmatism takes place after the nappe stacking events are induced by continental collision. Magma infiltrates both the underlying (East European) and overthrust plates (Tisia-Dacia). The magmas exploit the least resistance zones created by the collisional brittle fragmentation of the crusts. As several studies suggest, in this context magma generation is induced by slab break-off and associated asthenosphere rise (Mason et al., 1998; Seghedi et al., 1998; Wortel and Spakman, 2000). The development of plumbing systems, subvolcanic intrusions, and volcanic edifices are strongly controlled by tectonic processes, both in terms of location (along and at fault intersections) and in terms of the southward migration of the volcanism. This migration is coeval with the southward intra-mountain basin development. There is a clear tectonic control on magmatic input.

The structural control on the post-collisional CGH volcanic range shows some resemblances to “arc volcanism”, but also major differences. The magmatism is in both cases dominantly calc-alkaline, developed along a convergent plate boundary and involves extensional, strike-slip, and oblique tectonic movements. For the “arc” scenario, regional or local extension enhances the magmatic output more or less equally along the “arc” (e.g. Acocella, 2014 and references therein). However, in the post-collisional setting of the CGH, the tectonic regime changes in time. This occurs in respect to the evolution of the collisional front southwards, beyond the Trotuş fault (transition from the East European to the Moesian plate). As a result, not only the magma compositions change, but the magmatic output rates decrease strongly. For example, the extruded volumes decrease from an average of 19 $km^3$/Ma down to 7.7 $km^3$/Ma in the southern, younger volcanoes (Table 1). The decrease in erupted volumes correlates with the emplacement of smaller intrusions and smaller magma reservoirs towards the south. Hence, any future volcanism in the southern part of the CGH will likely erupt reduced volumes of magma.

The study also highlights an interesting gravimetric anomaly in the Transylvanian Basin, which has extensions towards the shallower geophysical environment. Whether this is related to a magmatic source is debatable and can generate potential research questions.

We trust that this paper highlights the need for future research on the close connection between magmatic and tectonic processes. In addition to providing valuable regional information, this could help to better assess similarities and differences between “arc volcanism” and “post-collisional” volcanism on a global scale.

## Acknowledgments

This work was supported by a grant of the Ministry of Education and Scientific Research, CNCS-UEFISCDI, project number PN-II-IDPCE-2012-4-0137 and by grant of Ministry of Research and Innovation, CNCS–UEFISCDI, project number PN-III-P4-ID-PCCF-2016-4-0014, within PNCDI III. We thank Mehmet Keskin and an anonymous reviewer for constructive comments that have improved the quality of this paper and Editor Kei Hirose for editorial handling.

## References

Acocella, V., 2014. Structural control on magmatism along divergent and convergent plate boundaries: overview, model, problems. Earth Sci. Rev. 136, 226–288.

Airinei St., Stoenescu S., Velcescu G., 1969. Geomagnetic maps ΔZ and ΔZa, scale 1:200.000, printed by Geological and Geofisical Institute (presently Geological Institute of Romania).

Balázs, A., Maţenco, L., Magyar, I., Horváth, F., Cloetingh, S., 2016. The link between tectonics and sedimentation in back-arc basins: new genetic constraints from the analysis of the Pannonian Basin. Tectonics. https://doi.org/10.1002/2015TC004109.

Bottrill, A.D., van Hunen, J., Allen, M.B., 2012. Insight into collision zone dynamics from topography: numerical modelling results and observations. Solid Earth 3, 387–399.

Chung, S.-L., Chu, M.F., Zhang, Y., Xie, Y., Lo, C.-H., Lee, T.-Y., Lan, C.-Y., Li, X., Zhang, Q., Wang, Y., 2005. Tibetan tectonic evolution inferred from spatial and temporal variations in post-collisional magmatism. Earth-Science Reviews 68, 3–4, 2005, Pages 173–196.

Cloetingh, S., Burov, E.B., 2011. Lithospheric folding and sedimentary basin evolution: a review and analysis of formation mechanisms. Basin Res. 23, 257–290.

Cloetingh, S.A.P.L., Burov, E., Maţenco, L., Toussaint, G., Bertotti, G., Andriessen, P.A.M., Wortel, M.J.R., Spakman, W., 2004. Thermo-mechanical controls on the mode of continental collision in the SE Carpathians (Romania). Earth Planet. Sci. Lett. 218, 57–76.

Demetrescu, C., Nielsen, S.B., Enea, M., Şerban, D.Z., Polonic, G., Andreescu, M., Pop, A., Balling, N., 2001. Lithosphere thermal structure and evolution of the Transylvanian depression — insights from new geothermal measurements and modelling results. Phys. Earth Planet. Inter. 126, 249–267.

Dilek, Y., Altunkaynak, S., 2007. Cenozoic crustal evolution and mantle dynamics of postcollisional magmatism in western. Anatolia: International. Geology Review 49, 431–453. https://doi.org/10.2747/0020-6814.49.5.431.

Doglioni, C., Carminati, E., Cuffaro, M., Scrocca, D., 2007. Subduction kinematics and dynamic constraints. Earth Sci. Rev. 83 (3–4), 125–175.

Erwan, T., Finlay, C.C., Beggan, C.D., Alken, P., Aubert, J., Barrois, O., Bertrand, F., Bondar, T., Boness, A., Brocco, L., Canet, E., Chambodut, A., Chulliat, A., Coïsson, P., Civet, F., Du, A., Fournier, A., Fratter, I., Gillet, N., Hamilton, B., Hamoudi, M., Hulot, G., Jager, T., Korte, M., Kuang, W., Lalanne, X., Langlais, B., Léger, J.-M., Lesur, V., Lowes, F.J., Macmillan, S., Mandea, M., Manoj, C., Maus, S., Olsen, N., Petrov, V., Ridley, V., Rother, M., Sabaka, T.J., Saturnino, D., Schachtschneider, R., Sirol, O., Tangborn, A., Thomson, A., Tøffner-Clausen, L., Vigneron, P., Wardinski, I., Zvereva, T., 2015. International Geomagnetic Reference Field: the 12th Generation.

Faccenna, C., Civetta, L., D'Antonio, M., Funiciello, F., Margheriti, L., Piromallo, C., 2005. Constraints on mantle circulation around the deforming Calabrian slab. Geophys. Res. Lett. 32, L06311. https://doi.org/10.01029/02004GL021874.

Fedele L., Seghedi I., Chung S-L., Laiena F., Lin Te-H., Morra V. Lustrino M. 2016. Post-

collisional magmatism in the Late Miocene Rodna-Bârgău district (East Carpathians, Romania): geochemical constraints and petrogenetic models. Lithos 266–267, 367–382.
Fielitz, W., Seghedi, I., 2005. Late Miocene–quaternary volcanism, tectonics and drainage system evolution in the East Carpathians, Romania. Tectonophysics 410, 111–136.
Gröger, H.R., Fugenschuh, B., Tischler, M., Schmid, S.M., Foeken, J.P.T., 2008. Tertiary cooling and exhumation history in the Maramureş area (internal eastern Carpathians, northern Romania): thermochronology and structural data. Geol. Soc. London Spec. Publ. 298 (1), 169–195.
Harangi, S., Downes, H., Seghedi, I., 2006. Tertiary–Quaternary subduction processes and related magmatism in Europe. In: Gee, D.G., Stephenson, R.A. (Eds.), European Lithosphere Dynamics. 32. Geological Society London Memoirs, pp. 167–190.
Hébert, R., Guilmette, C., Dostal, J., Bezard, R., Lesage, G., Bédard, É., Wang, C., 2014. Miocene post-collisional shoshonites and their crustal xenoliths, Yarlung Zangbo suture zone southern Tibet: geodynamic implications. Gondwana Res. 25, 1263–1271.
Heuret, A., Lallemand, S., 2005. Plate motions slab dynamics and back-arc deformation. Phys. Earth Planet. Inter. 149, 31–51.
Hinze, W.J., Von Frese, R.B., Saad, A.H., 2013. Gravity and Magnetic Exploration. Principles, Practices and Applications. 512 Cambridge University Press.
Horváth, F., Musitz, B., Balázs, A., Végh, A., Uhrin, A., Nádor, A., Koroknai, B., Pap, N., Tóth, T., Wórum, G., 2015. Evolution of the Pannonian basin and its geothermal resources. Geothermics 53, 328–352. https://doi.org/10.1016/j.geothermics.2014.07.009.
Ismail-Zadeh, A., Maţenco, L., Radulian, M., Cloetingh, S., Panza, G., 2012. Geodynamics and intermediate-depth seismicity in Vrancea (the south-eastern Carpathians): current state-of-the art. Tectonophysics 530–531, 50–79. https://doi.org/10.1016/j.tecto.2012.01.016.
Jolivet, L., Brun, J.-P., 2010. Cenozoic geodynamic evolution of the Aegean. Int. J. Earth Sci. 99, 109–138.
Jolivet, L., et al., 2013. Aegean tectonics: strain localisation, slab tearing and trench retreat. Tectonophysics 597–598, 1–33. doi:https://doi.org/10.1016/j.tecto.2012.06.011.
Karátson, D., Timár, G., 2005. Comparative volumetric calculations of two segments of the neogene/quaternary volcanic chain using SRTM elevation data: implications for erosion and magma output rates. Z. Geomorphol. Suppl. 140, 19–35.
Krézsek, C., Bally, A.W., 2006. The Transylvanian Basin (Romania) and its relation to the Carpathian fold and thrust belt: insights in gravitational salt tectonics. Mar. Pet. Geol. 23 (4), 405–442.
Liegeois, J.P., 1998. Preface-some words on the post-collisional magmatism. Lithos 45, xv–xvii.
Mason, P., Downes, H., Seghedi, I., Szakács, A., Thirlwall, M.F., 1995. Low-pressure evolution of magmas from the Călimani, Gurghiu and Harghita mountains. Acta Vulcanol. 7, 43–53.
Mason, P., Downes, H., Thirlwall, M.F., Seghedi, I., Szakács, A., Lowry, D., Mattey, D., 1996. Crustal assimilation as a major petrogenetic process in the east Carpathian Neogene and Quaternary continental margin arc, Romania. J. Petrol. 37, 927–959.
Mason, P.R.D., Seghedi, I., Szakács, A., Downes, H., 1998. Magmatic constraints on geodynamic models of subduction in the Eastern Carpathians, Romania. Tectonophysics 297, 157–176.
Maţenco, L., 2017. Tectonics and exhumation of Romanian Carpathians: inferences from kinematic and thermochronological studies. In: Rădoane, M., Vespremeanu-Stroe, A. (Eds.), Landform Dynamics and Evolution in Romania. Springer Geography, pp. 15–56. https://doi.org/10.1007/978-3-319-32589-7_2.
Maţenco, L., Bertotti, G., 2000. Tertiary tectonic evolution of the external East Carpathians (Romania). Tectonophysics 316, 255–486.
Maţenco, L., Radivojević, D., 2012. On the formation and evolution of the Pannonian Basin: constraints derived from the structure of the junction area between the Carpathians and Dinarides. Tectonics, 31. TC 6007. https://doi.org/10.1029/2012TC003206.
Maţenco, L., Zoetemeijer, R., Cloetingh, S., Dinu, C., 1997. Lateral variations in mechanical properties of the Romanian external Carpathians: inferences of flexure and gravity modelling. Tectonophysics 282, 147–166.
Maţenco, L., Krézsek, C., Merten, S., Schmid, S., Cloetingh, S., Andriessen, P., 2010. Characteristics of collisional orogens with low topographic build-up: an example from the Carpathians. Terra Nova 22, 155–165.
Milsom, J., Eriksen, A., 2011. Field Geophysics, Fourth edition. 287 Wiley-Blaclwell.
Molnár, K., Lukács, R., Dunkl, I., Schmitt, A.K., Kiss, B., Seghedi, I., Szepesi, J., Harangi, S., 2019. Episodes of dormancy and eruption of the Late Pleistocene Ciomadul volcanic complex (Eastern Carpathians, Romania) constrained by zircon geochronology. J. Volcanol. Geotherm. Res. 373, 133–147.
Okay, A.I., Sengor, A.M.C., Gorur, N., 1994. Kinematic history of the opening of the Black Sea and its effect on the surrounding regions. Geology 22 (3), 267–270.
Panaiotu, C.E., Vasiliev, I., Panaiotu, C.G., Krijgsman, W., Langereis, C.G., 2007. Provenance analysis as a key to orogenic exhumation: a case study from the East Carpathians (Romania). Terra Nova 19, 120–126.
Panaiotu, C.G., Vişan, M., Tugui, A., Seghedi, I., Panaiotu, A.G., 2012. Palaeomagnetism of the South Harghita volcanic rocks of the East Carpathians: implications for tectonic rotations and palaeosecular variation in the past 5Ma. Geophys. J. Int. 189, 369–382.
Pécskay, Z., Edelstein, O., Seghedi, I., Szakács, A., Kovacs, M., Crihan, M., Bernad, A., 1995. K–Ar datings of the Neogene-Quaternary calcalkaline volcanic rocks in Romania. In: Downes, H. & Vaselli, O. (eds) Neogene and related volcanism in the Carpatho-Pannonian region. Acta Vulcanol. 7, 53–63.
Pécskay, Z., Lexa, J., Szakács, A., Seghedi, I., Balogh, K., Konečný, V., Zelenka, T., Kovacs, M., Póka, T., Fülöp, A., Márton, E., Panaiotu, C., Cvetković, V., 2006. Geochronology of Neogene–Quaternary magmatism in the Carpathian arc and Intra-Carpathian area: a review. Geol. Carpath. 57, 511–530.
Prelević, D., Seghedi, I., 2013. Magmatic response to the post-accretionary orogenesis within alpine–Himalayan belt—preface. Lithos 181, 1–4.
Reeves, C., 1995. Aeromagnetic Survey, Principles, Practice & Interpretation. (Published by Geosoft).
Royden, L.H., 1993. Evolution of retreating subduction boundaries formed during continental collision. Tectonics 12 (3), 629–638.
Sanders, C. A. E., Andriessen, P. A. M., Cloetingh, S. A. P. L., 1999. Life cycle of the East Carpathian orogen: Erosion history of a doubly vergent critical wedge assessed by fission track thermochronology. J. Geophys. Res. 104 (B12), 29, 095–29, 112.
Sanders, C., Huismans, R., van Wees, J.D., Andriessen, P., 2002. The Neogene history of the Transylvanian basin in relation to its surrounding mountains. In: Cloetingh, S., Horvath, F., Bada, G., Lankreijer, A. (Eds.), Neotectonics and Surface Processes: The Pannonian Basin and Alpine/Carpathian System. vol. 3. EGU Special Publication, pp. 121–133.
Săndulescu, M., 1984. Geotectonica, României. Ed. Tehnica, Bucharest (In Romanian). (366 pp).
Schmid, S., Bernoulli, D., Fügenschuh, B., Maţenco, L., Schefer, S., Schuster, R., Tischler, M., Ustaszewski, K., 2008. The Alpine–Carpathian–Dinaridic orogenic system: correlation and evolution of tectonic units. Swiss J. Geosci. 101, 139–183.
Seghedi, I., Downes, H., 2011. Geochemistry and tectonic development of Cenozoic magmatism in the Carpathian–Pannonian region. Gondwana Res. 20, 655–672.
Seghedi, I., Szakács, A., Stanciu, C., Ioane, D., 1994. Neogene arc volcanicity/metallogeny in the Călimani-Gurghiu-Harghita volcanic Mts. In field trip guide “Plate tectonics and metallogeny in the East Carpathians and Apuseni Mts.”. Geol. Inst. Romania 12–17.
Seghedi, I., Balintoni, I., Szakács, A., 1998. Interplay of tectonics and Neogene post-collisional magmatism in the intracarpathian area. Lithos 45, 483–499.
Seghedi, I., Downes, H., Szakács, A., Mason, P.R.D., Thirlwall, M.F., Roşu, E., Pécskay, Z., Marton, E., Panaiotu, C., 2004a. Neogene–quaternary magmatism and geodynamics in the Carpathian–Pannonian region: a synthesis. Lithos 72, 117–146.
Seghedi, I., Szakács, A., Snelling, N., Pécskay, Z., 2004b. Evolution of the Neogene Gurghiu Mountains volcanic range (eastern Carpathians, Romania), based on K-Ar geochronology. Geol. Carpath. 55 (4), 325–332.
Seghedi, I., Maţenco, L., Downes, H., Mason, P.R.D., Szakács, A., Pécskay, Z., 2011. Tectonic significance of changes in post-subduction Pliocene–Quaternary magmatism in the south east part of the Carpathian–Pannonian Region. Tectonophysics 502, 146–157.
Seghedi, I., Popa, R.-G., Panaiotu, C.G., Szakács, A., Pécskay, Z., 2016. Short-lived eruptive episodes during the construction of a Na-alkalic basaltic field (Perşani Mountains, SE Transylvania, Romania). Bull. Volcanol. 78, 69. https://doi.org/10.1007/s00445-016-1063-y.
Seghedi, I., Szakács, A., Mirea, V., Vişan, M., Luffi, P., 2017. Challenges of mapping in poorly-exposed volcanic areas. Guide and abstracts, Romanian Journal of Earth Sciences, vol 91, Special Issue, (90 pp).
Silva, J.B.C., 1986. Reduction to the pole as an inverse problem and its application to low latitude anomalies. Geophysics 51, 369–382.
Szakács, A., Krezsék, C., 2006. Volcano-basement interaction in the Eastern Carpathians: explaining unusual tectonic features in the Eastern Transylvanian Basin, Romania. J. Volcanol. Geotherm. Res. 158, 6–20.
Szakács, A., Seghedi, I., 1995. The Călimani–Gurghiu–Harghita volcanic chain, East Carpathians, Romania: volcanological features. Acta Volcanol 7, 145–153.
Szakács, A., Seghedi, I., 1996. Volcaniclastic sequences around andesitic stratovolcanoes, East Carpathians, Romania, Workshop guide, of the IAVCEI, CEV and CVS commisions. Rom. Jour. of Petrology 77, 55p supplement 1.
Szakács, A. and Seghedi, I., 2000. Large volume volcanic debris avalanche in the East Carpathians, Romania. In Volcaniclastic rocks, from magma to sediments, H. Leyrit and C. Montenat (edt), Ed. Gordon Breach Science Publishers, 131–151.
Szakács, A., Seghedi, I., Pécskay, Z., 1993. Pecularities of South Harghita Mts. as terminal segment of the Carpathian Neogene to Quaternary volcanic chain. Rev. Roum. de Géol. 37, 21–36.
Szakács A., Ioane D., Seghedi I., Rogobete M., Pécskay Z., 1997. Rates of migration of volcanic activity and magma output along the Calimani-Gurghiu-Harghita volcanic range, East Carpathians, Romania. PANCARDI’97, Prz. Geol. 45, 10/2: 1106.
Szakács, A., Seghedi, I., Pécskay, Z., Mirea, V., 2015. Eruptive history of a low-frequency and low-output rate Pleistocene volcano, Ciomadul, South Harghita Mts. Romania. Bull. Volcanol. 77, 12. https://doi.org/10.1007/s00445-014-0894-7.
Tărăpoancă, M., Bertotti, G., Maţenco, L., Dinu, C., Cloetingh, S., 2003. Architecture of the Focşani depression: a 13 km deep basin in the Carpathians bend zone (Romania). Tectonics 22 (6), 1074. https://doi.org/10.1029/2002TC001486.
Tari, G., Dovenyi, P., Dunkl, I., Horváth, F., Lenkey, L., Ştefănescu, M., Szafian, P., Toth, T., 1999. Lithospheric structure of the Pannonian basin derived from seismic, gravity and geothermal data. Geological Society London Special Publication 156, 215–250.
Toussaint, G., Burov, E., Avouac, J.-P., 2004. Tectonic evolution of a continental collision zone: a thermo mechanical numerical model. Tectonics 23, TC6003. https://doi.org/10.1029/2003TC001604.
Ustaszewski, K., Schmid, S., Fügenschuh, B., Tischler, M., Kissling, E., Spakman, W., 2008. A map-view restoration of the Alpine–Carpathian–Dinaridic system for the

Early Miocene. Swiss J. Geosci. 101, 273–294.
Uyeda, S., Kanamori, H., 1979. Back-arc opening and the mode of subduction. J. Geophys. Res. 84, 1049–1061.
Vergés, J., Fernàndez, M., 2012. Tethys-Atlantic interaction along the Iberia-Africa plate boundary: the Betic-Rif orogenic system. Tectonophysics 579, 144–172. https://doi.org/10.1016/j.tecto.2012.08.032.
Vişan, M., Panaiotu, C.G., Necula, C., Dumitru, A., 2016. Palaeomagnetism of the Upper Miocene-Lower Pliocene lavas from the East Carpathians: contribution to the paleosecular variation of geomagnetic field. Sci. Rep. 6, 23411. https://doi.org/10.1038/srep23411.
Wortel, M.J.R., Spakman, W., 2000. Subduction and slab detachment in the Mediterranean–Carpathian region. Science 290, 1910–1917.
Zhang, W.–.X., Zhu, L.–.Q., Wang, H., Wu, Y.–.B., 2018. Generation of post-collisional normal calc-alkaline and adakitic granites in the Tongbai orogen, Central China. Lithos 296–299, 513–531.